

International Journal of Modern Physics D
© World Scientific Publishing Company

**Dynamics of wide binary stars: A case study for testing Newtonian
dynamics in the low acceleration regime**

Riccardo Scarpa

*Instituto de Astrofísica de Canarias, c/via Lactea s/n
San Cristobal de la Laguna, 38205, Spain*

*Departamento de Astrofísica, Universidad de La Laguna (ULL), 38206 La Laguna, Tenerife,
Spain*

riccardo.scarpa@gtc.iac.es

Riccardo Ottolina

*Dipartimento di Scienza e Alta Tecnologia, Università degli Studi dell'Insubria, via Valleggio 11
Como, 22100, Italy*

Renato Falomo

*Osservatorio Astronomico di Padova, INAF, vicolo dell' Osservatorio 5
Padova, 35122, Italy*

renato.falomo@oapd.inaf.it

Aldo Treves

*Dipartimento di Scienza e Alta Tecnologia, Università degli Studi dell'Insubria, via Valleggio 11
Como, 22100, Italy*

aldo.treves@uninsubria.it

Received Day Month Year

Revised Day Month Year

Extremely wide binary stars represent ideal systems to probe Newtonian dynamics in the low acceleration regimes ($< 10^{-10} \text{ m s}^{-2}$) typical of the external regions of galaxies. Here we present a study of 60 alleged wide binary stars with projected separation ranging from 0.004 to 1 pc, probing gravitational accelerations well below the limit where dark matter or modified dynamics theories set in. Radial velocities with accuracy $\sim 100 \text{ m/s}$ were obtained for each star, in order to constrain their orbital velocity, that, together with proper motion data, can distinguish bound from unbound systems. It was found that about half of the observed pairs do have velocity in the expected range for bound systems, out to the largest separations probed here. In particular, we identified five pairs with projected separation $> 0.15 \text{ pc}$ that are useful for the proposed test. While it would be premature to draw any conclusion about the validity of Newtonian dynamics at these low accelerations, our main result is that very wide binary stars seem to exist in the harsh environment of the solar neighborhood. This could provide a tool to test Newtonian dynamics versus modified dynamics theories in the low acceleration conditions typical of galaxies. In the near future the GAIA satellite will provide data to increase significantly the number of wide pairs that, with the appropriate follow up spectroscopic observations,

2 *Scarpa et al.*

will allow the implementation of this experiment with unprecedented accuracy.

Keywords: Gravitation - Star binary:general

PACS numbers: 04.50.Kd, 95.35.+d, 97.10.Vm, 97.80.-d,

1. Introduction

A wealth of astronomical data indicate the dynamics in a variety of classes of cosmic structures deviate from the expectation of Newtonian dynamics applied to the mass visible in stars and gas. These observations are usually explained invoking the existence of vast amounts of unseen mass in some novel form, dark matter (e.g. Refs. 1, 2). Alternatively the data could be interpreted as a breakdown of Newtonian dynamics on the relevant regime. While most investigators would agree that the former is the correct explanation, an increasing number of empirical results support the latter (e.g. Ref. 3 for a recent review). In particular, the proliferation of alternative theories of dynamics found nowadays in the literature points to the presence of an acceleration scale — $a_0 \sim 10^{-10} \text{ m s}^{-2}$ — above which classical dynamics is recovered and below which the dark matter mimicking regime appears.

The vast majority of the work on alternative theories of gravity was focused on explaining the dynamical properties of galaxies, most notably the detailed shape their flat rotation curve, e.g. Ref. 4.

When modifying gravity in the low-acceleration regime, the strong equivalence principle is in general broken, and systems embedded in a stronger field than their internal gravitational field might not display a modified gravity behaviour. However, this is not the case for any possible theory of modified dynamics, as shown by, e.g., 5): it is thus conceivable that the modified dynamics regime kicks in below a given acceleration scale independently of the external field. According to this, in the past years we tested Newtonian dynamics using stars in globular clusters (See Refs. 6-9), which due to their small size are believed to contain negligible amount of dark matter, if any. It was found that the orbital velocities of stars in their outskirts, where $a < a_0$, are too large to be consistent with Newtonian dynamics. A result that has been corroborated for a growing number of globular clusters by various independent groups (e.g. Refs. 10,11). The interpretation of this result is, however, complicated by a number of effects that could mimic the modified dynamics behavior — cluster evaporation, tidal heating, peculiar orbital motion, uncertain mass-to-light ratio, dark remnants — thus preventing to draw a clear cut conclusion.

In order to carry out a cleaner test, free from contaminating external effects, one might look at the simplest stellar system: wide binary stars. Indeed, sufficiently wide binaries could probe the acceleration regime typical of galaxies, thus permitting a direct test of Newtonian dynamics below a_0 .

For a test particle orbiting around a $1M_\odot$ star, modified gravity supposedly sets in at separation of $r_0 \sim 7000 \text{ AU}$ (0.03 pc), and the expected orbital velocity is $\sim 250 \text{ m/s}$. This separation is so large and the orbital velocity so low that at the time of writing, there is no hope to directly trace the orbital motion. Indeed, it is not even clear whether such wide binaries can exist at all in the harsh environment nearby the Sun, where tidal effects and close encounter with other stars could destroy them (see e.g. Ref. 12).

Assuming that such wide binaries exist and have a stable orbit — a hypothesis corroborated by detailed numerical simulations showing that the effects on wide binaries of the Milky Way external field do not alter the Keplerian fall-off at least up to separations of the Jacobi radius, which in the solar vicinity is $\sim 1.7 \text{ pc}$ (Ref. 12) — the gravitational acceleration can be constrained measuring the instantaneous orbital velocity of the two components. Considering a large sample of binaries, uniformly covering a wide range of separations, it is then possible to trace the run of velocity with distance, in this way building the equivalent of a galaxy rotation curve. Compared to other experiments, the use of binary stars has the major advantage that the masses involved are known from

their spectral type, thus removing one important source of uncertainty (the mass-to-light ratio), making this test one of the cleanest possible.

Therefore since double stars are not surrounded by an halo of dark matter, Newtonian dynamics predicts this “rotation curve” must fall off as $v \propto r^{-1/2}$, essentially following Kepler’s third law, provided the range of masses is small. On the contrary, if the velocity converges toward a relatively large, constant value as seen in galaxies, then we will be forced to seriously question our understanding of Newton’s law of gravity in low acceleration regimes.

In the case only one or two components of the velocity vector is known, projection effects play an important role and the Newtonian predictions become an upper limit to the observed velocity. A preliminary attempt to carry out a test of this kind was performed by Hernandez et al. (Ref. 13). They discuss the difference of orbital velocity derived from Hipparcos proper motion for a large sample of binaries, suggesting that the orbital velocity might *not* decrease with the star separation. Unfortunately, the data discussed by Hernandez et al. (Ref. 13) have large uncertainties (average error on velocity 0.8 km/s) making their result rather weak and inconclusive. Moreover, not having information about the radial velocity of these stars, the proper motion data alone leave open the possibility that a significant fraction of the stars under consideration are not gravitationally bound even though the proper motion data suggest so.

Here we present results of a first attempt to cope with this last problem. A number of alleged wide double stars — selected mostly according to Hipparcos parallaxes and proper motion data — were observed spectroscopically to derive their radial velocity with accuracy of $\sim 100 \text{ m s}^{-1}$ so to build their 3d velocity vector and to confirm the velocity difference of the two components is small, as it should be for bound systems. As we will see, while most alleged doubles are not confirmed as such by the new data, a number of them are consistent with the hypothesis of being bound systems, making this test feasible.

2. What are the expectations?

2.1. The case of standard Newtonian dynamics

Let assume a double star with components of mass m_1 and m_2 , separated by $S = r_1 + r_2$, where r_1 and r_2 are the distances of each star from the center of mass of the system. Equating the momentum $m_1 r_1 = m_2 r_2$ of the two masses with respect to the center of mass we obtain:

$$r_1 = \frac{S m_2}{m_1 + m_2} \quad (1)$$

and a similar expression for r_2 . Assuming for simplicity circular orbit, equating centripetal acceleration to gravitational acceleration on m_1 :

$$\frac{v_1^2}{r_1} = \frac{G m_2}{S^2} \quad (2)$$

where v_1 is the velocity of component 1, which becomes:

$$v_1^2 = \frac{G m_2^2}{S(m_1 + m_2)}. \quad (3)$$

and a similar expression for v_2 . In the simplest case where $m_1 = m_2 = m$ and consequently $v_1 = v_2 = v$ we further get

$$v^2 = \frac{G m}{2S}. \quad (4)$$

This last expression gives the expected orbital velocity for each star. However, because the two components of a pair are moving in opposite directions, the *observed* velocity difference ΔV is twice as large. Thus, calling $m_{tot} = 2m$ the total mass of the system, we finally have:

$$\Delta V_{observed} = \sqrt{\frac{G m_{tot}}{S}} \quad (5)$$

4 *Scarpa et al.*

The resulting orbital velocity for two stars of $1M_{\odot}$ each and separation $S = 7000$ AU is 250 m/s, with a corresponding *observed* $\Delta V \sim 500$ m/s. This value corresponds to the 3d velocity vector. When considering only the radial velocity, projection effects and orbital ellipticity will play a role, making this an upper limit to the radial velocity difference we should expect to observe. Whatever the case, the orbital velocity should decrease with separation.

2.2. Expectations for modified dynamics

An alternative approach to the missing mass problem is to replace dark matter by a modified dynamics theory. In the literature various approaches have been proposed. The best known of them being the MODified Newtonian Dynamics (MOND) or its relativistic version called TensorVectorScalar (TeVeS) theory (Refs. 14 - 15). Another example is the generally covariant MODified Gravity (MOG) theory (Ref. 18). Some successful attempt to apply quantum gravity to galaxies were also made (Ref. 19), or by introducing non-local gravity (Ref. 20).

Here, to quantify the effects of modified dynamics we adopt, for its simplicity, the MOND working formula with the standard interpolation function (Refs. 14-17). In doing so, we assign no special value to MOND compared to the others theories, in particular because due to the external field effect, MOND as a modified gravity formula should not be directly applicable to systems surrounded by a strong external field, as is the case of stars inside the Milky Way (Ref. 14), though the effects we are looking for in this work could actually be present in some version of MOND (5).

According to MOND formula for acceleration of gravity well below $a_0 = 1.2 \times 10^{-10}$ m s⁻², the acceleration should become

$$a = \sqrt{a_N a_0} \quad (6)$$

where a_N is the usual Newtonian acceleration. Therefore for the simplest case of a double star with equal mass components and circular orbits outlined above we can write:

$$\frac{v}{S} = \sqrt{\frac{Gm_{tot}a_0}{4S^2}} \quad (7)$$

from which one immediately gets

$$v = \left(\frac{Gm_{tot}a_0}{4} \right)^{1/4}. \quad (8)$$

The most important aspect of this relation is that the separation of the two stars disappeared, so that the orbital velocity becomes constant. This behavior is similar to what is observed in rotation curves of galaxies. That is, MOND-like formulae suggest that for separations larger than ~ 7000 AU the orbital velocity should be constant with asymptotic value of ~ 300 m/s in the case of $1M_{\odot}$ stars, and a corresponding *observed* ΔV twice as big. The dependence on the mass is very weak, thus this limit applies to all double stars considered in this study, which have masses in the range $0.4 < m < 1.5$ solar masses. Since in Newtonian dynamics the orbital velocity keeps decreasing, the difference between the two scenarios becomes significant at larger separations (lower acceleration). For instance, at 0.1 pc separation, the predicted orbital velocity is twice the Newtonian value.

3. The sample of wide binary stars candidates.

Wide binary star candidates were selected from the Shaya & Olling catalogue (Ref. 21). In this catalog wide binaries are identified by assigning a probability above chance alignment for each system, with probability obtained using a sophisticated Bayesian statistical analysis in a multi-dimensional parameter space of proper motions and spatial positions of the Hipparcos catalog (Ref. 22).

From the Shaya & Olling catalogue we selected isolated binaries with a probability of non-chance alignment greater than 99%. The binary search criteria used by the authors require that the proposed binary should have no near neighbors; the projected separation between the two components is thus always many times smaller than the typical interstellar separation, which is very important for our test. It is also important to note the catalogue includes both “presently bound” and “previously bound” pairs. Previously bound pairs are those which according to the authors have been destroyed by the Galactic tidal field and perturbation from nearby stars (Ref. 12). Considering we are testing a scenario of modified dynamics, having also these “previously bound” stars ensure we are not missing precisely those systems moving too fast for Newton but not for modified dynamics.

In summary we select pairs from the catalogue according to the following criteria:

- stars are classified as double, not multiple;
- probability of the pair to be physically bound (or previously bound) greater than 99%;
- mass between 0.4 and 1.5 solar masses;
- pair projected separation smaller than 1.5 pc;
- declination $> -40^\circ$ for good visibility from Roque de los Muchachos observatory (La Palma);
- both stars in the pair are not known to be spectroscopic binary;
- relative error on the distance $< 15\%$.

This selection yielded 60 pairs of stars (see Table 1) in the magnitude range $4 < V < 12$, and distances going from 14 pc to 100 pc. Note that when referring to the distance of a pair we mean the average distance of the two components. The 55% of the sample stars are within 50 pc with associated errors on distance of few parsecs. Apparent separations of selected stars range from 30 to 3650 arcsec, which according to distance correspond to projected physical separation in the 0.004 to 1.3 pc range, most of the pairs being within 0.1 pc separation. As mentioned before we are interested in the behavior of binaries with separation above $r_0 = 7000$ AU, that is 0.034 pc, while smaller separations will be used to check whether the Newtonian dynamics is recovered. The sample includes 29 and 31 pairs with separation smaller and larger than this value, respectively.

Table 1: The selected sample (horizontal lines separate different pairs).

Legend:

NH = Hipparcos catalogue star number;

RA = Right ascension;

DEC = Declination;

V = Apparent V band magnitude;

ST = Spectral type;

d = Distance from parallax;

pmRA = Proper motion along RA in milliarcsec/year;

pmDEC = Proper motion along DEC in milliarcsec/year.

NH	RA [hh:mm:ss]	DEC [dd:mm:ss]	V	ST	d [pc]	pmRA [msec/yr]	pmDEC [msec/yr]
185	00:02:21.64	10:47:08.32	8.5	F8	77.4 ± 5.5	-45.33 ± 1.61	-115.73 ± 1.09
190	00:02:25.33	10:46:35.95	8.7	G0	87.5 ± 7.1	-49.43 ± 1.06	-118.65 ± 0.79
201	00:02:33.44	18:41:00.11	8.2	F5	92.2 ± 8.9	-13.19 ± 0.70	17.41 ± 0.56
206	00:02:35.24	18:50:09.58	8.6	G0	99.9 ± 9.6	-18.50 ± 0.78	19.70 ± 0.59
1891	00:23:53.20	29:30:09.10	8.2	G	84.6 ± 7.5	41.80 ± 1.18	-3.47 ± 0.82
1887	00:23:51.46	29:29:45.29	8.5	G	71.9 ± 4.9	39.41 ± 1.30	0.11 ± 0.90
2292	00:29:16.18	-05:54:35.82	7.8	G0	56.7 ± 2.5	-113.02 ± 1.07	-220.86 ± 0.68
2350	00:29:59.93	-05:45:48.45	9.4	G5	49.9 ± 3.7	-107.08 ± 1.51	-224.06 ± 0.91

Continued on next page

Table 1 – continued from previous page

NH	RA [hh:mm:ss]	DEC [dd:mm:ss]	V	ST	d [pc]	pmRA [msec/yr]	pmDEC [msec/yr]
4702	01:00:27.93	-19:23:21.33	8.0	G3V	74.7 ± 5.1	127.66 ± 1.02	-54.14 ± 0.67
4833	01:02:06.82	-19:40:10.35	8.3	G3V	86.9 ± 6.5	129.62 ± 1.04	-54.00 ± 0.69
8497	01:49:35.19	-10:41:10.25	4.7	F3III	23.2 ± 0.1	-148.90 ± 0.87	-94.47 ± 0.86
8486	01:49:23.43	-10:42:11.93	6.7	G0	22.6 ± 1.5	-122.64 ± 4.36	-100.38 ± 4.09
10321	02:12:54.96	40:40:06.98	7.2	G0V	26.8 ± 0.4	59.29 ± 0.71	-108.78 ± 0.67
10339	02:13:13.29	40:30:28.16	7.3	G0V	26.2 ± 0.4	58.11 ± 0.65	-95.90 ± 0.76
11137	02:23:19.40	15:25:05.21	8.9	G5	58.8 ± 4.6	112.85 ± 1.68	185.66 ± 1.11
11134	02:23:17.03	15:24:59.62	9.4	G5	57.1 ± 5.4	111.79 ± 2.09	185.42 ± 1.33
11783	02:32:05.28	-15:14:39.55	4.7	F5V	26.7 ± 0.2	-80.92 ± 0.69	-146.84 ± 0.64
11759	02:31:42.52	-15:16:23.39	8.7	K2.5Vk	27.9 ± 0.7	-75.71 ± 1.29	-120.03 ± 1.36
15304	03:17:26.29	07:39:20.97	7.4	F8V	46.1 ± 2.0	169.30 ± 1.66	-7.64 ± 0.96
15310	03:17:32.68	07:41:24.61	7.8	G0	41.8 ± 2.1	170.41 ± 1.93	-7.48 ± 1.10
15527	03:20:03.35	-28:51:14.09	7.4	G1.5V	35.5 ± 0.8	348.88 ± 0.50	-64.82 ± 0.73
15526	03:20:02.71	-28:47:01.21	8.5	G9.5V	35.4 ± 1.4	349.07 ± 0.78	-67.80 ± 1.00
17118	03:39:58.64	63:52:14.74	6.8	F5	42.5 ± 0.9	129.42 ± 0.58	-143.11 ± 0.66
17126	03:40:05.21	63:52:29.81	8.2	G5	40.7 ± 1.7	137.58 ± 0.94	-131.99 ± 1.04
19335	04:08:36.50	38:02:24.82	5.5	F7V	21.0 ± 0.1	163.93 ± 0.65	-203.52 ± 0.55
19255	04:07:34.22	38:04:30.31	7.1	G5	20.4 ± 0.3	172.94 ± 1.01	-226.60 ± 0.89
19859	04:15:28.86	06:11:13.64	6.3	G0IV	21.3 ± 0.2	-109.37 ± 1.12	-108.35 ± 1.12
19855	04:15:25.85	06:11:59.73	6.9	G5IV	21.1 ± 0.3	-101.62 ± 1.16	-112.85 ± 1.15
20342	04:21:28.68	-20:54:55.48	8.8	K2.5V	38.6 ± 2.2	190.51 ± 1.33	130.36 ± 1.36
20338	04:21:26.29	-20:54:06.56	11.5	K9V _k	30.8 ± 3.8	197.15 ± 2.52	141.96 ± 3.16
20669	04:25:40.26	63:40:29.47	8.3	G0	62.4 ± 2.9	-128.25 ± 0.90	-55.73 ± 0.98
20637	04:25:22.84	63:37:34.70	10.0	K0	64.3 ± 6.3	-128.46 ± 1.62	-51.39 ± 1.96
21537	04:37:26.71	00:33:11.13	7.5	G5	66.9 ± 3.2	17.23 ± 1.20	11.42 ± 0.95
21534	04:37:26.08	00:34:28.57	7.5	G5	66.1 ± 3.4	15.21 ± 1.17	12.90 ± 0.95
21704	04:39:37.02	-21:14:51.36	7.2	K0/K1I	87.1 ± 5.9	12.96 ± 0.95	21.67 ± 0.95
21702	04:39:34.95	-21:14:23.14	9.0	G0	90.9 ± 13.1	13.01 ± 1.26	22.20 ± 1.30
22611	04:51:54.19	-34:14:19.25	6.7	F6IV/V	59.3 ± 1.4	75.89 ± 0.45	9.10 ± 0.54
22604	04:51:47.90	-34:13:17.27	8.8	G5V	57.6 ± 2.7	73.75 ± 0.70	7.86 ± 0.86
24046	05:10:03.74	27:33:24.20	7.0	F8V	40.0 ± 1.3	197.69 ± 1.11	-88.54 ± 0.59
24035	05:10:00.74	27:38:36.24	9.2	G5	39.7 ± 1.9	207.69 ± 1.54	-84.28 ± 0.80
25278	05:24:25.31	17:23:00.79	5.0	F8V	14.4 ± 0.1	250.40 ± 0.88	-7.42 ± 0.61
25220	05:23:38.23	17:19:26.87	7.9	K2	14.1 ± 0.3	253.35 ± 1.21	-4.66 ± 0.76
33705	07:00:09.76	-31:08:30.38	6.6	F5.5VF	37.4 ± 0.5	19.70 ± 0.58	34.37 ± 0.64
33691	07:00:02.73	-31:13:41.42	8.4	G9V	37.1 ± 1.2	20.44 ± 0.82	35.10 ± 0.93
34426	07:08:12.02	15:31:16.91	7.7	F8	45.9 ± 1.6	-56.97 ± 1.04	-212.48 ± 0.81
34407	07:08:00.27	15:31:44.75	7.8	G0V	46.8 ± 1.9	-51.42 ± 1.07	-206.54 ± 0.84
34714	07:11:19.56	33:06:42.78	7.2	F5	48.2 ± 1.4	-111.55 ± 1.62	-8.00 ± 0.85
34700	07:11:14.80	32:36:54.12	8.0	G0	45.2 ± 1.6	-110.82 ± 1.32	-5.71 ± 0.79
39457	08:03:53.84	-31:32:40.62	8.7	G3V	73.3 ± 6.2	-74.05 ± 0.95	148.61 ± 1.08
39452	08:03:50.71	-31:33:06.99	9.7	-	71.3 ± 10.0	-70.51 ± 6.29	143.46 ± 7.40
40918	08:21:03.76	65:26:33.58	8.0	G0	36.5 ± 1.2	24.63 ± 0.74	21.56 ± 0.72
40882	08:20:33.34	65:23:38.11	8.4	G5	37.3 ± 1.6	11.65 ± 0.85	21.55 ± 0.84
44520	09:04:15.04	03:01:35.71	8.9	G5	56.2 ± 4.9	58.67 ± 1.56	-92.23 ± 0.77
44518	09:04:13.87	03:02:02.72	9.3	G5	47.8 ± 4.0	48.12 ± 1.87	-87.70 ± 0.92
44858	09:08:23.90	27:32:06.96	8.2	G0V	47.1 ± 2.9	-52.32 ± 1.43	70.25 ± 1.01
44864	09:08:27.19	27:32:34.62	8.3	G0V	42.6 ± 2.0	-52.19 ± 1.45	73.24 ± 1.02
45811	09:20:29.03	-09:33:20.27	4.8	G8III-	68.2 ± 1.4	-13.42 ± 0.90	-26.80 ± 0.57
45802	09:20:21.02	-09:36:36.37	7.0	F4V	62.8 ± 2.7	-14.57 ± 1.21	-30.04 ± 0.78

Continued on next page

Table 1 – continued from previous page

NH	RA [hh:mm:ss]	DEC [dd:mm:ss]	V	ST	d [pc]	pmRA [msec/yr]	pmDEC [msec/yr]
45836	09:20:43.79	51:15:56.57	6.1	F3V	27.4 ± 0.4	-34.76 ± 0.72	145.35 ± 0.46
45859	09:21:03.04	51:18:20.41	7.8	G5	28.3 ± 0.6	-37.21 ± 0.91	141.23 ± 0.54
47436	09:39:57.85	35:20:09.42	6.9	F5	49.0 ± 1.1	-67.95 ± 0.81	2.97 ± 0.55
47403	09:39:28.10	35:14:35.13	7.1	F5	49.0 ± 1.2	-68.06 ± 0.87	2.38 ± 0.59
50325	10:16:38.12	41:16:33.23	7.4	F5	55.8 ± 1.8	23.71 ± 0.73	-18.18 ± 0.67
50327	10:16:39.13	41:18:19.80	8.7	F8	50.1 ± 2.3	23.27 ± 0.92	-21.44 ± 0.78
52787	10:47:31.23	-22:20:52.67	8.4	K0V	34.5 ± 1.0	-122.67 ± 0.93	-29.38 ± 0.91
52776	10:47:25.47	-22:17:11.91	9.9	K4.5Vk	32.6 ± 1.5	-125.57 ± 1.55	-30.45 ± 1.25
54692	11:11:49.05	42:49:57.67	7.2	F8	46.8 ± 1.3	-130.55 ± 0.65	-237.88 ± 0.66
54681	11:11:37.75	42:49:05.46	8.3	G5	48.4 ± 1.9	-117.50 ± 0.85	-242.43 ± 0.81
57858	11:51:57.57	08:49:48.42	7.4	K0	96.5 ± 6.7	-9.68 ± 1.10	-50.69 ± 0.73
57856	11:51:56.54	08:49:21.97	7.9	K0III-	98.9 ± 7.7	-1.48 ± 1.23	-52.75 ± 0.80
58067	11:54:32.35	19:24:40.57	8.2	G0	40.5 ± 1.8	-450.28 ± 1.40	-14.27 ± 1.01
58073	11:54:35.36	19:25:40.31	8.4	G5	38.4 ± 2.0	-452.68 ± 1.32	-15.39 ± 1.15
58751	12:02:59.82	-10:45:08.45	7.4	F5	59.2 ± 2.2	33.82 ± 0.73	-18.37 ± 0.60
58722	12:02:39.44	-10:42:48.94	8.5	G0	55.1 ± 3.0	33.59 ± 0.92	-17.81 ± 0.72
64057	13:07:39.88	24:00:34.03	8.2	G5V	35.4 ± 1.2	-260.82 ± 1.07	148.28 ± 0.81
64059	13:07:40.90	24:01:10.47	8.6	G0	37.3 ± 1.7	-261.79 ± 1.15	146.19 ± 0.92
64444	13:12:32.07	-34:44:50.60	7.8	F5/F6V	77.0 ± 6.9	-250.44 ± 1.28	-270.47 ± 1.56
64443	13:12:30.40	-34:45:14.27	9.8	K0	58.8 ± 7.5	-244.24 ± 2.99	-274.78 ± 2.46
65602	13:27:03.12	-24:17:25.06	8.7	K2+v	29.4 ± 0.7	-337.25 ± 1.34	-61.08 ± 0.70
65574	13:26:39.77	-24:17:35.52	8.8	K2.5Vk	30.2 ± 1.0	-335.87 ± 1.57	-70.65 ± 0.83
65899	13:30:30.77	22:30:47.47	8.6	F8	76.2 ± 5.2	27.20 ± 1.08	-45.48 ± 0.65
65884	13:30:18.97	21:30:01.38	10.0	G5	71.9 ± 6.4	20.33 ± 1.55	-49.68 ± 0.85
66749	13:40:50.75	-17:47:33.53	7.9	F3V	85.1 ± 4.7	-35.86 ± 1.05	-11.49 ± 0.66
66717	13:40:32.53	-17:20:37.30	8.5	F3V	85.7 ± 6.2	-46.34 ± 1.39	-13.34 ± 0.65
67250	13:46:59.87	38:32:33.90	5.5	K0III+	97.2 ± 3.1	-134.18 ± 0.47	-21.69 ± 0.45
67041	13:44:20.40	38:47:52.05	8.9	G5	95.2 ± 9.6	-141.29 ± 0.72	-21.72 ± 0.75
68830	14:05:38.54	-18:04:20.08	8.2	F8+...	80.6 ± 7.2	41.70 ± 1.41	-44.51 ± 1.08
68833	14:05:38.92	-18:04:50.92	8.8	G0	78.2 ± 7.3	37.18 ± 1.80	-44.64 ± 1.59
69701	14:16:00.88	-05:59:58.29	4.1	F7IV	22.2 ± 0.1	-25.84 ± 0.91	-419.84 ± 0.68
69962	14:18:58.28	-06:36:09.34	9.1	K7V	21.8 ± 0.8	-5.17 ± 1.89	-432.05 ± 1.29
71726	14:40:18.33	30:26:38.20	7.7	G0	53.5 ± 1.7	95.06 ± 0.89	-44.25 ± 0.77
71737	14:40:28.34	30:31:14.23	8.0	G2IV	51.3 ± 2.4	95.59 ± 1.06	-44.78 ± 0.86
74442	15:12:47.73	27:55:36.72	8.4	G0V	79.8 ± 5.5	9.63 ± 1.10	-131.12 ± 0.93
74439	15:12:45.92	27:55:15.21	9.4	G0	69.1 ± 6.4	7.13 ± 1.69	-131.25 ± 1.41
74666	15:15:30.10	33:18:54.37	3.5	G8III	37.3 ± 0.2	84.84 ± 0.37	-110.57 ± 0.48
74674	15:15:38.29	33:19:16.28	7.8	G0Vv	37.0 ± 1.0	83.89 ± 0.52	-109.54 ± 0.68
85620	17:29:44.45	63:51:11.15	7.7	F9V	45.2 ± 1.0	2.48 ± 0.63	-182.16 ± 0.67
85575	17:29:16.58	63:52:10.49	8.4	G0	45.2 ± 1.1	0.31 ± 0.72	-181.38 ± 0.77
96895	19:41:49.09	50:31:31.61	6.0	G1.5Vb	21.1 ± 0.1	-147.75 ± 0.56	-158.85 ± 0.50
96901	19:41:52.10	50:31:04.51	6.2	G3V	21.2 ± 0.1	-135.15 ± 0.60	-163.53 ± 0.52
97295	19:46:25.58	33:43:43.28	5.0	F7V	21.2 ± 0.1	23.05 ± 0.42	-448.66 ± 0.50
97222	19:45:33.52	33:36:11.00	7.7	K3V	21.1 ± 0.4	13.30 ± 1.07	-440.57 ± 1.35
99729	20:14:09.85	06:35:20.83	7.7	G4IV	61.1 ± 4.6	-132.91 ± 1.57	-60.63 ± 1.84
99727	20:14:09.26	06:34:38.49	8.0	G4V	61.4 ± 5.2	-130.02 ± 1.74	-61.72 ± 2.06
101082	20:29:27.31	81:05:26.66	6.0	K0III+	63.7 ± 0.9	67.05 ± 0.62	221.67 ± 0.55
101166	20:30:21.65	81:08:20.21	8.7	G5	68.9 ± 2.4	67.54 ± 0.87	221.35 ± 0.81
101916	20:39:07.59	10:05:10.15	5.1	G5IV+	30.1 ± 0.3	323.58 ± 0.82	21.07 ± 0.55
101932	20:39:21.86	10:04:32.46	8.5	K2V	28.7 ± 0.7	317.09 ± 1.27	20.21 ± 0.84

Continued on next page

Table 1 – continued from previous page

NH	RA [hh:mm:ss]	DEC [dd:mm:ss]	V	ST	d [pc]	pmRA [msec/yr]	pmDEC [msec/yr]
110419	22:21:57.60	-34:31:12.96	7.4	F4V	86.2 ± 7.7	9.87 ± 1.21	25.83 ± 0.85
110433	22:22:04.58	-34:29:20.30	7.5	F2/F3I	74.0 ± 4.2	9.65 ± 1.13	26.62 ± 0.68
112222	22:43:42.69	10:56:23.23	6.5	G8IV	42.4 ± 3.0	9.80 ± 1.11	-171.17 ± 1.25
112354	22:45:27.86	11:11:32.43	9.8	K6V:	41.6 ± 2.8	13.82 ± 2.96	-162.90 ± 2.92
112970	22:52:42.16	67:59:24.04	7.0	F2	59.0 ± 1.5	78.49 ± 0.67	63.42 ± 0.61
112946	22:52:30.05	67:59:36.49	7.5	F5	59.9 ± 1.4	80.88 ± 0.56	59.22 ± 0.52
113579	23:00:19.22	-26:09:12.09	7.5	G5V	30.8 ± 0.7	108.87 ± 1.02	-160.41 ± 0.74
113597	23:00:27.88	-26:18:41.38	9.6	K7V	30.5 ± 1.9	113.63 ± 2.65	-162.16 ± 2.11
117573	23:50:37.98	54:11:53.91	7.1	F5	58.5 ± 2.2	-2.18 ± 0.54	-34.03 ± 0.55
117733	23:52:39.67	54:16:08.14	7.6	F5	55.9 ± 2.0	-5.13 ± 0.64	-39.66 ± 0.67
118254	23:59:08.97	41:12:06.25	7.7	G0	44.3 ± 1.3	80.21 ± 0.68	4.40 ± 0.51
118251	23:59:06.80	41:10:13.97	8.2	G0	41.9 ± 1.1	82.20 ± 0.70	3.56 ± 0.52

4. Observations and data reduction

Observations were gathered during two separated observing runs, in January and December 2013, at the 2.5 m Nordic Optical Telescope, located at the Roque de los Muchachos observatory, in the Canary islands. Radial velocities were obtained with the fiber feed FIES Echelle spectrograph (Ref. 23), in high resolution mode ($R = \lambda/\Delta\lambda = 67000$) plus simultaneous calibration lamp to achieve the highest velocity accuracy. Atmospheric conditions were below average (poor seeing) during observations, nevertheless targets were bright enough to ensure spectra with sufficiently high signal to noise spectra for our purpose could be gathered within minutes. Note that to ensure the best stability the FIES spectrograph is sitting in a dedicated protected room, and is linked to the telescope by an optical fiber. Moreover, in all cases, the two components of a given pair were observed consecutively one after the other within minutes, ensuring environmental variation (e.g., pressure and temperature) had no effect.

Data have been reduced using the FIES pipeline (Ref. 24). The pipeline performs the standard reduction, bias subtraction, flat fielding, identification of the spectra position and extraction, combination of the different orders, wavelength calibration using a separate calibration frame and, finally, it uses the footprint of the simultaneous calibration lamp to compensate for any wavelength instability in the spectrograph.

5. Spectral analysis

The crucial aspect of our analysis is the measurement of the radial velocity of the selected stars. To do this we performed cross-correlation (task FXCOR in IRAF) of the observed stellar spectrum with an appropriate template. Synthetic template spectra were extracted from the BLUERED library^a, an extended theoretical library of synthetic stellar spectra (Ref. 25), covering the optical range from 3500 to 7000 Å at a spectral resolving power $R = 50000$. The library is based on the ATLAS9 model atmospheres (Ref. 26). The grid spans a large volume in three-dimensional parameters space: the effective temperature ranges from 4000 to 50,000 K and the surface gravity spans from 0.0 to 5.0 dex at six different solar-scaled metallicity values ($[M/H] = -3.0, -2.0, -1.0, -0.3, +0.0, +0.3$). Template-spectra were degraded to $R=70000$ to match the resolution of the data. Examples of observed spectra and the associated templates are shown in fig. 1. Metallicity has marginal influence in the templates, thus we assume solar metallicity for all spectra. The association of the template to each observed spectrum was based on the spectral type of the star and we checked the similarity by visual inspection.

^a<http://inaoep.mx/modelos/bluered/bluered.html>

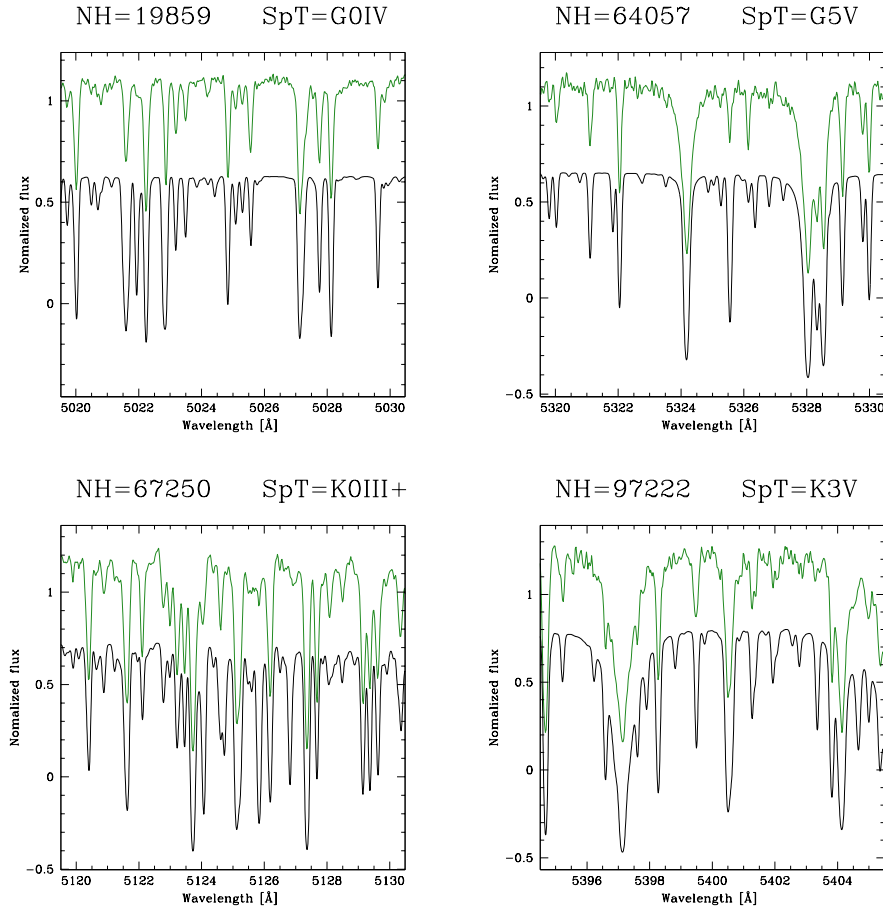


Fig. 1. Examples of observed spectrum (green top spectrum) with the adopted stellar synthetic template (black bottom spectrum) for stars of various spectral type.

In a number of cases the observed spectra exhibit absorption lines that are much wider than expected for the corresponding spectral type. This broadening of the lines is interpreted as due to fast rotation of the star. An effect most evident in stars of spectral type F5 or earlier. To cope with this problem templates were convolved with a Gaussian kernels of various sizes to match the observed line width (Fig. 2). The final cross-correlation with the modified template spectrum did work well, though the measurements of the radial velocity have somewhat larger errors in these cases.

5.1. Analysis

For each spectrum, cross-correlation was performed in spectral intervals of 200 \AA between 4100 \AA and 6700 \AA to derive the radial velocity (RV) of the stars. Excluding the spectral regions contaminated by telluric absorption bands, there are 13 suitable intervals, resulting in 13 values of RV.

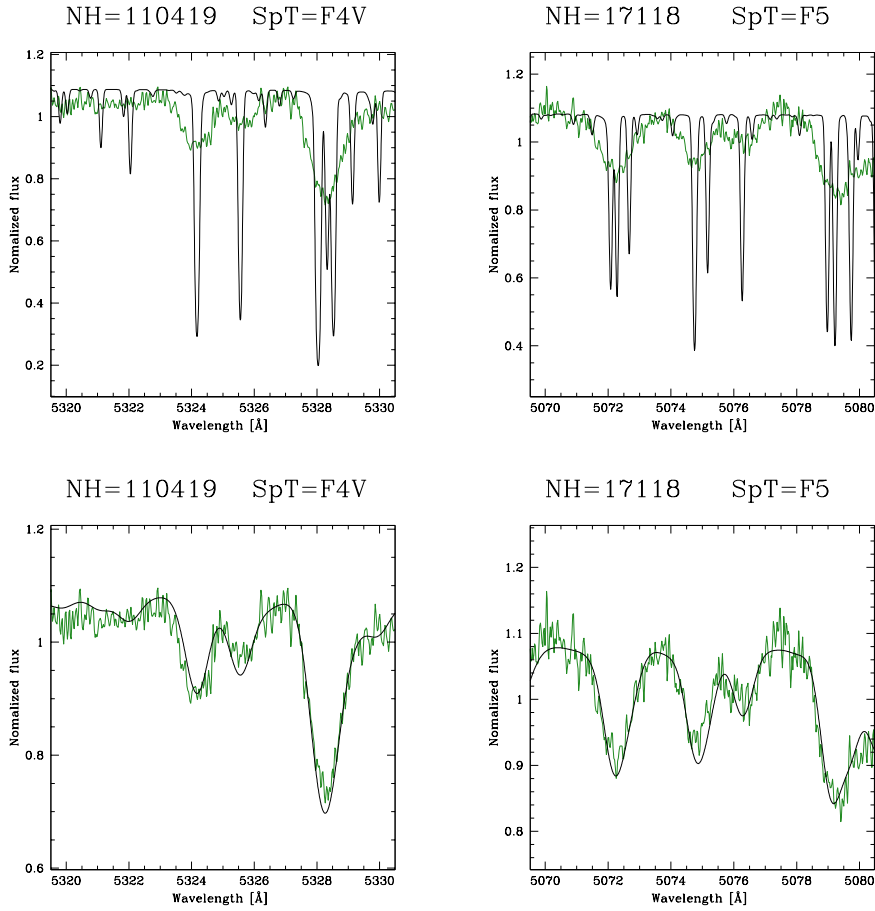


Fig. 2. Upper panels: Example of observed spectrum (green) compared to the best associated template (black) before convolution to compensate for the star rotation. The difference in line width is apparent. Lower panels: Spectra and template after convolution to match line width.

Then, for each interval, the measured RV was retained according to the following criteria:

- correlation peak greater than 0.5;
- error on RV smaller than 2σ from the average error (of the other intervals);
- RV within 5σ from average of RV (σ -clipping).

In all cases at least 8 out of 13 values could be retained. The final RV associated to each star was then computed as the weighted mean of these values. Tests were made to check whether our measurements could be sensitive to small changes in the selected template. No such effect was found. The final velocities, corrected to heliocentric reference frame, are given in Table 2.

Table 2: Table of results (horizontal lines separate different pairs).

Legend:

NH = Hipparcos catalogue star number;**MJD** = Modified julian date of observation;**expt** = Exposure time in seconds;**RV** = Measured heliocentric radial velocity in km/s.

NH	MJD [day]	expt [s]	RV [km/s]
185	56643.924	350	0.830 ± 0.016
190	56643.931	400	0.505 ± 0.014
201	56644.877	600	3.969 ± 0.058
206	56644.888	700	3.659 ± 0.080
1891	56324.829	200	-24.515 ± 0.019
1887	56324.836	300	-20.508 ± 0.015
2292	56324.844	200	10.105 ± 0.014
2350	56324.851	600	9.854 ± 0.018
4702	56644.931	400	5.647 ± 0.012
4833	56644.940	450	6.103 ± 0.014
8497	56643.959	120	-1.814 ± 0.250
8486	56643.964	220	-4.905 ± 0.013
10321	56324.881	200	7.252 ± 0.014
10339	56324.887	200	7.037 ± 0.018
11137	56643.987	500	27.129 ± 0.014
11134	56643.996	600	27.286 ± 0.016
11783	56644.008	90	-26.254 ± 0.018
11759	56644.013	500	-27.912 ± 0.021
15304	56324.915	250	31.860 ± 0.019
15310	56324.921	300	32.716 ± 0.019
15527	56644.950	350	40.287 ± 0.019
15526	56644.960	550	40.664 ± 0.014
17118	56324.930	200	17.006 ± 0.177
17126	56324.936	400	12.288 ± 0.043
19335	56323.825	60	26.461 ± 0.054
19335	56324.945	70	26.498 ± 0.055
19255	56323.834	120	27.846 ± 0.016
19255	56324.950	250	28.030 ± 0.017
19859	56323.842	90	-6.858 ± 0.012
19855	56323.848	90	-7.430 ± 0.016
20342	56324.961	500	78.756 ± 0.016
20338	56645.020	1200	89.218 ± 0.057
20669	56323.854	150	-35.784 ± 0.026
20637	56323.864	600	-36.285 ± 0.017
21537	56323.913	150	38.947 ± 0.016
21534	56323.919	150	39.082 ± 0.015
21704	56644.064	400	8.374 ± 0.026
21702	56644.073	600	8.417 ± 0.015
22611	56645.056	250	46.203 ± 0.015
22604	56645.063	500	46.444 ± 0.016
24046	56323.925	120	15.889 ± 0.022
24046	56324.977	300	16.001 ± 0.024
24035	56323.930	480	7.666 ± 0.023
24035	56324.989	900	7.775 ± 0.023

Continued on next page

Table 2 – continued from previous page

NH	MJD [day]	expt [s]	RV [km/s]
25278	56323.941	45	38.350 ± 0.047
25220	56323.945	200	38.603 ± 0.023
33705	56644.130	150	16.700 ± 0.027
33691	56644.139	600	17.141 ± 0.017
34426	56325.042	300	-11.552 ± 0.019
34426	56644.150	400	-11.538 ± 0.017
34407	56325.050	300	-12.309 ± 0.018
34407	56644.163	400	-12.350 ± 0.014
34714	56325.057	350	3.196 ± 0.020
34714	56646.121	900	3.196 ± 0.018
34700	56325.064	500	3.490 ± 0.021
34700	56646.139	1200	3.364 ± 0.017
39457	56645.111	500	26.807 ± 0.015
39452	56645.121	600	27.548 ± 0.016
40918	56323.978	200	8.402 ± 0.017
40918	56645.147	500	5.953 ± 0.014
40882	56323.986	300	2.741 ± 0.018
40882	56645.157	550	2.749 ± 0.015
44520	56325.115	600	5.461 ± 0.015
44520	56646.176	900	6.626 ± 0.016
44518	56325.128	700	7.474 ± 0.016
44518	56646.190	1000	6.461 ± 0.018
44858	56324.021	250	30.478 ± 0.015
44858	56645.214	500	30.469 ± 0.014
44864	56324.028	250	30.746 ± 0.017
44864	56645.223	500	30.781 ± 0.015
45811	56325.140	60	25.246 ± 0.014
45811	56644.241	200	25.312 ± 0.013
45802	56325.144	150	36.886 ± 0.091
45802	56644.247	400	-2.116 ± 0.071
45836	56324.035	90	-7.789 ± 0.016
45836	56645.200	120	-7.730 ± 0.017
45859	56324.039	200	-6.436 ± 0.014
45859	56645.205	400	-6.414 ± 0.013
47436	56325.180	120	6.288 ± 0.031
47436	56646.229	300	6.272 ± 0.030
47403	56325.185	300	-34.218 ± 0.017
47403	56646.236	600	-36.193 ± 0.018
50325	56324.046	150	10.812 ± 0.032
50327	56324.055	300	12.289 ± 0.015
52787	56325.219	250	24.212 ± 0.019
52776	56325.225	500	24.622 ± 0.022
54692	56324.081	150	11.727 ± 0.015
54692	56645.233	400	11.665 ± 0.015
54681	56324.088	250	10.346 ± 0.014
54681	56645.242	600	10.341 ± 0.013
57858	56325.234	120	-4.031 ± 0.013
57856	56325.238	150	-3.601 ± 0.048
58067	56325.243	200	6.461 ± 0.015
58073	56325.248	200	6.320 ± 0.014
58751	56324.101	250	-12.248 ± 0.041

Continued on next page

Table 2 – continued from previous page

NH	MJD [day]	expt [s]	RV [km/s]
58722	56324.107	300	-15.411 ± 0.020
64057	56324.116	300	-1.247 ± 0.014
64059	56324.123	500	-1.264 ± 0.013
64444	56325.254	120	-8.575 ± 0.027
64443	56325.258	500	-3.156 ± 0.021
65602	56644.285	400	-12.884 ± 0.018
65574	56644.294	450	-11.870 ± 0.018
65899	56324.134	500	-35.396 ± 0.019
65884	56324.144	900	57.917 ± 0.015
66749	56324.248	300	-7.355 ± 0.195
66749	56325.277	120	-7.909 ± 0.055
66717	56324.255	400	-0.809 ± 0.031
66717	56325.282	240	-0.913 ± 0.036
67250	56324.233	60	-10.781 ± 0.014
67250	56325.296	60	-10.776 ± 0.014
67041	56324.237	500	-32.428 ± 0.012
67041	56325.300	150	-32.393 ± 0.012
68830	56324.203	300	22.022 ± 0.280
68833	56324.210	480	28.301 ± 0.016
69701	56324.264	60	12.155 ± 0.041
69962	56324.269	600	11.817 ± 0.041
71726	56324.281	200	-11.468 ± 0.015
71737	56324.288	480	-11.298 ± 0.015
74442	56646.248	600	-60.207 ± 0.016
74439	56646.259	900	-59.245 ± 0.016
74666	56646.273	90	-11.844 ± 0.013
74674	56646.277	700	-11.477 ± 0.017
85620	56644.815	350	-33.736 ± 0.027
85575	56644.824	450	-33.294 ± 0.021
96895	56644.800	200	-27.455 ± 0.011
96901	56644.809	200	-27.043 ± 0.011
97295	56644.787	90	4.769 ± 0.023
97222	56644.794	200	5.124 ± 0.015
99729	56644.833	450	-0.011 ± 0.018
99727	56644.842	650	-0.072 ± 0.019
101082	56643.813	200	-14.069 ± 0.014
101166	56643.820	200	-13.747 ± 0.014
101916	56643.827	120	-53.457 ± 0.015
101932	56643.832	180	-53.118 ± 0.016
110419	56645.804	600	-15.719 ± 0.204
110433	56645.816	700	-14.754 ± 0.245
112222	56643.841	120	-5.597 ± 0.033
112354	56643.846	350	-1.038 ± 0.047
112970	56643.863	200	2.348 ± 0.146
112946	56643.870	250	1.758 ± 0.025
113579	56644.854	450	7.022 ± 0.041
113597	56644.863	800	52.181 ± 0.113
117573	56643.893	300	14.113 ± 0.110
117573	56645.862	600	13.951 ± 0.125
117733	56643.900	350	15.314 ± 0.020

Continued on next page

Table 2 – continued from previous page

NH	MJD [day]	expt [s]	RV [km/s]
117733	56645.895	700	15.346 ± 0.023
118254	56643.909	300	30.368 ± 0.016
118251	56643.916	350	29.621 ± 0.014

For 14 pairs (28 stars) two spectra were obtained at different epochs to confirm the stability of our measurements and/or possibly identify stars that, for whatever reason, do have variable radial velocity. It was found that about half of these stars indeed have variable velocity well above statistical uncertainties. The other half shows remarkable stability, with mean velocity difference between repeated measurements of 62 ± 9 m/s, confirming the good quality of the data.

Finally, radial velocity standard stars were observed to check the radial velocity zero point of the instrument. Specifically, we obtained spectra of HD38230 and HD50692 twice in two consecutive nights, finding consistent radial velocity within few tens of m/s. There is, however, a statistically significant offset of 378 ± 46 m/s in the zero point when compared with catalogue values. While we cannot find a simple explanation for this offset, our main result remain unaffected by this, because we are only interested in *differences* of radial velocity.

6. Results

The observed radial velocity difference ΔV_r for our 60 pairs is reported in Table 3 and shown in Fig.3 as a function of projected separation. For comparison, the tangential component ΔV_{PM} from Hipparcos proper motions is also shown. The difference between the two plots is striking, with approximately 50% of the pairs having radial velocity clearly incompatible with the pairs being bound systems (in any reasonable scenario). It is clear, however, that a bias is present because stars with large proper motion difference would have not entered in the Shaya & Olling catalog in the first place. Therefore, adding accurate radial velocities give us immediately the possibility to show that either something alter the velocity of the stars, or many systems are unbound in spite of the high probability to be bound assigned solely according to proper motion data.

Table 3: Table of difference in radial velocities.

Legend:

NH1 = Number of Hipparcos catalogue of the first star;**NH2** = Number of Hipparcos catalogue of the second star;**sep** = Projected separation. The value is obtained from the angular separation multiplied by the weighted average of the parallaxes distances of the binary sistem;**dpm** = Difference in proper motion. The value is obtain combining the value of proper motion along two different direction;**dRV** = Difference in radial velocity. Δt = time interval between repeated observations in days

NH1	NH2	sep [pc]	dpm [msec/yr]	dRV [km/s]	Δt [Days]
185	190	0.0249 ± 0.0013	3.360 ± 1.800	0.325 ± 0.021	
201	206	0.2554 ± 0.0174	1.726 ± 1.597	0.310 ± 0.099	
1891	1887	0.0121 ± 0.0007	5.805 ± 1.656	-4.007 ± 0.024	
2292	2350	0.222 ± 0.0084	3.360 ± 1.865	0.251 ± 0.023	
4702	4833	0.6633 ± 0.0335	0.500 ± 1.900	-0.456 ± 0.018	

Continued on next page

Table 3 – continued from previous page

NH1	NH2	sep [pc]	dpm [msec/yr]	dRV [km/s]	Δt [Days]
8497	8486	0.0207 ± 0.0001	7.596 ± 11.135	3.091 ± 0.250	
10321	10339	0.0791 ± 0.0008	2.802 ± 1.600	0.215 ± 0.023	
11137	11134	0.0098 ± 0.0006	1.432 ± 1.400	-0.157 ± 0.021	
11783	11759	0.0449 ± 0.0003	2.184 ± 1.493	1.658 ± 0.028	
15304	15310	0.0333 ± 0.0011	3.734 ± 1.900	-0.856 ± 0.027	
15527	15526	0.0435 ± 0.0009	1.082 ± 2.596	-0.377 ± 0.024	
17118	17126	0.0094 ± 0.0002	3.413 ± 2.128	4.718 ± 0.182	
19335	19255	0.0758 ± 0.0003	22.064 ± 3.733	-1.385 ± 0.056	1.1
19335	19255	–	–	-1.532 ± 0.058	
19859	19855	0.0066 ± 0.0001	11.226 ± 2.139	0.572 ± 0.020	
20342	20338	0.0105 ± 0.0005	9.055 ± 3.200	-10.462 ± 0.059	
20669	20637	0.0638 ± 0.0027	4.880 ± 2.700	0.501 ± 0.031	
21537	21534	0.0252 ± 0.0009	5.324 ± 1.701	-0.135 ± 0.022	
21704	21702	0.0172 ± 0.0011	1.020 ± 3.396	-0.043 ± 0.030	
22611	22604	0.0285 ± 0.0006	4.254 ± 1.725	-0.241 ± 0.022	
24046	24035	0.0609 ± 0.0016	2.640 ± 1.600	8.223 ± 0.032	1.0
24046	24035	–	–	8.226 ± 0.033	
25278	25220	0.0493 ± 0.0003	7.033 ± 3.468	-0.253 ± 0.052	
33705	33691	0.0587 ± 0.0007	2.209 ± 1.799	-0.441 ± 0.032	
34426	34407	0.0386 ± 0.001	5.482 ± 1.400	0.757 ± 0.026	319.1
34426	34407	–	–	0.812 ± 0.022	
34714	34700	0.4069 ± 0.0091	0.608 ± 1.603	-0.294 ± 0.029	321.1
34714	34700	–	–	-0.168 ± 0.025	
39457	39452	0.0169 ± 0.0012	2.955 ± 3.200	-0.741 ± 0.022	
40918	40882	0.0461 ± 0.0012	1.393 ± 2.000	5.661 ± 0.025	321.1
40918	40882	–	–	3.204 ± 0.021	
44520	44518	0.008 ± 0.0005	5.738 ± 1.600	-2.013 ± 0.022	321.0
44520	44518	–	–	0.165 ± 0.024	
44858	44864	0.0111 ± 0.0004	4.123 ± 1.723	-0.268 ± 0.023	321.2
44858	44864	–	–	-0.312 ± 0.021	
45811	45802	0.0745 ± 0.0014	1.746 ± 1.300	-11.640 ± 0.092	319.1
45811	45802	–	–	27.428 ± 0.072	
45836	45859	0.031 ± 0.0004	4.386 ± 1.684	-1.353 ± 0.021	321.2
45836	45859	–	–	-1.316 ± 0.021	
47436	47403	0.1174 ± 0.0019	1.769 ± 1.947	40.506 ± 0.035	321.0
47436	47403	–	–	42.465 ± 0.035	
50325	50327	0.0279 ± 0.0007	0.943 ± 1.529	-1.477 ± 0.035	
52787	52776	0.0386 ± 0.0009	3.245 ± 3.031	-0.410 ± 0.029	
54692	54681	0.0309 ± 0.0007	7.203 ± 1.300	1.381 ± 0.021	321.2
54692	54681	–	–	1.324 ± 0.020	
57858	57856	0.0145 ± 0.0007	4.640 ± 2.000	-0.430 ± 0.050	
58067	58073	0.0141 ± 0.0005	3.206 ± 1.300	0.141 ± 0.021	
58751	58722	0.0927 ± 0.0028	2.417 ± 1.600	3.163 ± 0.046	
64057	64059	0.0068 ± 0.0002	2.377 ± 1.400	0.017 ± 0.019	
64444	64443	0.0105 ± 0.0008	1.526 ± 2.100	-5.419 ± 0.034	
65602	65574	0.0459 ± 0.0009	2.267 ± 2.632	-1.014 ± 0.025	
65899	65884	1.3181 ± 0.0714	5.292 ± 1.300	-93.313 ± 0.024	
66749	66717	0.6772 ± 0.0297	10.508 ± 1.900	-6.546 ± 0.197	1.0
66749	66717	–	–	-6.996 ± 0.066	
67250	67041	0.9788 ± 0.0298	5.869 ± 1.600	21.647 ± 0.018	1.0

Continued on next page

Table 3 – continued from previous page

NH1	NH2	sep [pc]	dpm [msec/yr]	dRV [km/s]	Δt [Days]
67250	67041	–	–	21.617 ± 0.018	
68830	68833	0.012 ± 0.0008	4.002 ± 2.000	-6.279 ± 0.280	
69701	69962	0.3682 ± 0.0016	12.462 ± 9.283	0.338 ± 0.058	
71726	71737	0.078 ± 0.0021	2.159 ± 2.195	-0.170 ± 0.021	
74442	74439	0.0118 ± 0.0007	2.596 ± 1.615	-0.962 ± 0.023	
74666	74674	0.019 ± 0.0001	1.720 ± 1.700	-0.367 ± 0.021	
85620	85575	0.0424 ± 0.0007	4.528 ± 1.700	-0.442 ± 0.034	
96895	96901	0.004 ± 0	15.728 ± 1.614	-0.412 ± 0.016	
97295	97222	0.0814 ± 0.0004	8.443 ± 5.466	-0.355 ± 0.027	
99729	99727	0.0128 ± 0.0007	2.717 ± 2.200	0.061 ± 0.026	
101082	101166	0.0669 ± 0.0009	0.316 ± 1.600	-0.322 ± 0.020	
101916	101932	0.031 ± 0.0003	4.880 ± 1.749	-0.339 ± 0.022	
110419	110433	0.0528 ± 0.0025	1.924 ± 1.603	-0.965 ± 0.319	
112222	112354	0.3654 ± 0.0178	13.788 ± 2.100	-4.559 ± 0.057	
112970	112946	0.02 ± 0.0003	1.082 ± 1.500	0.590 ± 0.148	
113579	113597	0.0867 ± 0.0019	8.645 ± 3.234	-45.159 ± 0.120	
117573	117733	0.3035 ± 0.0079	3.023 ± 1.769	-1.201 ± 0.112	2.0
117573	117733	–	–	-1.395 ± 0.127	
118254	118251	0.0239 ± 0.0005	2.594 ± 1.600	0.747 ± 0.021	

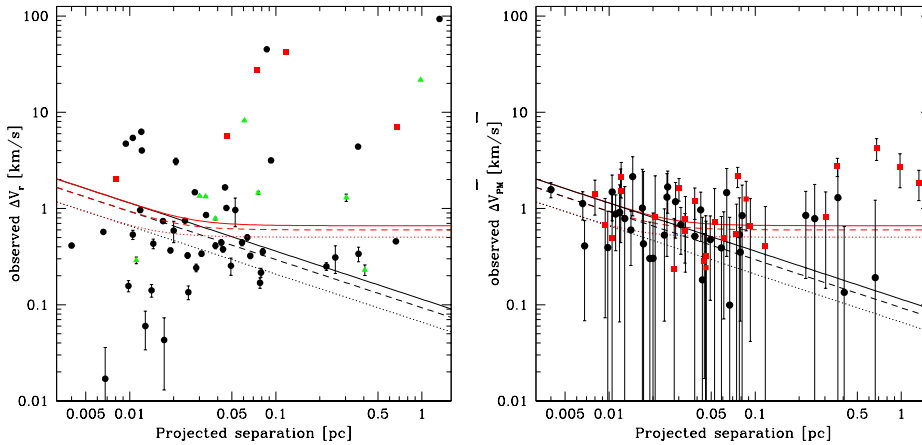


Fig. 3. The measured radial velocity difference as a function of the projected separation for the observed pairs. The black lines represent the relationship between total ΔV (not just the radial or tangential component) and star separation for binary stars with total mass of 1.0 (dotted line), 2.0 (dashed line) and 3.0 (filled line) solar masses. **Left:** The radial component of the observed velocity ΔV_r difference is twice the component of the orbital velocity. Error bars give the 1σ uncertainty, when not visible the error bar is smaller than the symbol. Stars observed twice are marked as red squares if ΔV_r did vary more than 3σ between observations, as triangles if ΔV_r remained constant within statistical errors. **Right:** The velocity difference along the tangential direction as derived from proper motions (filled circles). Note the error bars are significantly larger than those for radial velocity measurements. Points are black or red according to whether ΔV_r is below or above the MOND prediction for a three solar masses star pair, respectively.

The Newtonian and modified gravity upper limit velocity expectations are also reported. Note in our sample $3M_{\odot}$ is the very maximum *total* mass a pair can have, thus, if all pairs were bound all points should fall, as a minimum, below the modified dynamics prediction. As mentioned before, for 14 pairs (28 stars) we have repeated measurements. Scanning the velocity for these stars (Tab. 2), we identify 3 possible cases: the velocity of both stars in the pair varied, only one varied, neither varied. Here it is also important to take into account the time separation between observations, in our case either about 1-2 days or ~ 300 days.

For instance, pair 66749/66717, which was observed at 1 day distance, showed a substantial variation of the radial velocity of both stars (600 and 100 m/s). The most probable explanation for this variation in such a short amount of time is that both stars are themselves double (we are then dealing with a quadruple system) of which we are mapping the orbital velocity of two close internal binary systems. While pairs like this are still potentially useful for testing Newtonian dynamics, they require a substantial observational effort in order to average out these internal orbital variations. And the situation would be even worse if the internal systems are moderately wide, because in this case observations should cover a much longer period of time before velocity variation can be identified. We feel most of the points above the maximum theoretical limit belong to this class.

In pairs like 47436/47403 and 45811/45802 only one of the two stars has variable radial velocity. Again, the simplest explanation is that we are dealing with a triple system. Star 45802 is particularly striking, showing a change of about 40 km/s over a baseline of 319 days. Possibly, if observed at 1 day distance, this star will have shown a variation similar to the one of 66749. Also in this case a substantial observational effort is required to wash out the variations.

Finally, pairs 34426/34407, 44858/44864, 45836/45859, 54692/54681 observed over a large time baseline, do show constant velocity (within statistical uncertainties). These are the most interesting cases. Unfortunately we have only four of them (the remaining 5 pairs with stable velocity were observed at short time distance so the result is less significant).

Of the 50 pairs with projected separation < 0.15 pc, where Newtonian and modified dynamics made very similar predictions, 28 pairs are below the Newtonian upper limit for $3M_{\odot}$ pair (and one more below the modified gravity limit).

In view of what we found for the stars with repeated observations, a number of the systems below the Newtonian limit could be multiple. While it is possible that by chance these pairs have been observed in an orbital phase corresponding to a low velocity difference, we believe that this is unlikely. So we are confident that a substantial fraction of these 28 pairs are bound systems suitable for testing Newtonian dynamics.

Considering the remaining 10 pairs with separation > 0.15 pc one immediately notices the absence of systems below the Newtonian limits, while there are 5 pairs formally in agreement with the modified dynamics limit. The remaining 5 pairs have radial velocity > 1 km/s and must be either unbound or multiple systems. The 5 pairs sitting in the region between the two models are unquestionably the most interesting and certainly deserve further investigation.

7. Conclusions

We have shown that for about half of the observed pairs, accurate radial velocity measurements support the hypothesis that these pairs are indeed gravitationally bound systems. On the other hand the radial velocity data also show that about 50% of the pairs cannot be bound systems, making clear that proper motion data alone is not sufficient to perform the proposed test (Ref. 13). Moreover, repeated radial velocity measurements appear to be mandatory in order to further eliminate multiple systems of stars that

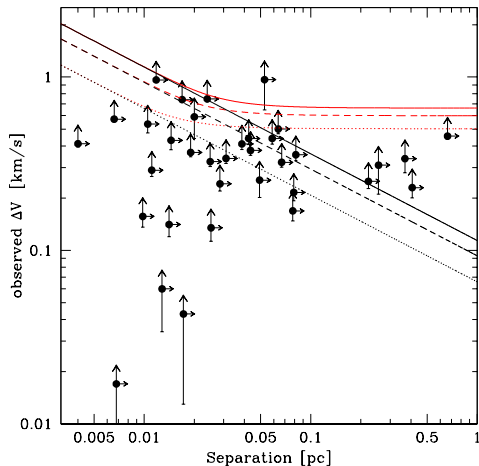


Fig. 4. The observed velocity difference vs the pair separation S for pairs with $\Delta V_r < 2$ km/s. The observed separation corresponds to a lower limit to the true one. A few points beyond 0.15 pc separations might correspond to gravitationally bound systems.

might have escaped detection in the proper motion data analysis.

With the present dataset, we can only point out that looking at the wider pairs, at least a few of them seem at odd with Newtonian prediction while remaining formally consistent with modified dynamics (see Figure 4). Since we are able to observe accurately only one component of the velocity difference and the real separation between the stars will be larger than that observed (namely the projected one), some additional pairs would probably move into this intermediate region when these effects will be taken into account (see Figure 4). While it is premature from this data to draw any conclusion about dynamics at low accelerations, it is worth to underline that our observations suggest the existence of very wide gravitationally bound binary stars in the solar neighborhood, making the proposed test feasible.

In the near future, the GAIA satellite (<http://sci.esa.int/gaia/>) will provide proper motion data with very high accuracy, also dramatically increasing the number of stars for which such data will be available. GAIA will provide limited radial velocity information. Still, these radial velocity data, while of insufficient quality for the proposed test, will prove extremely valuable for selecting wide pair candidates, dramatically reducing the number of false positive. Once selected according to proper motion and radial velocity, a minimum of two high resolution spectra with radial velocity accuracy ~ 100 m/s will have to be obtained for each component of the pair, in this way pinning down the third component of the velocity vector and eliminating stars that for whatever reasons have variable radial velocity. Our results suggest that once all these new data will be available, a sufficiently large number of extremely wide binaries will be identified, providing enough information to build the “rotation curve” of binary stars up to ~ 1 pc separation. This will probe in the cleanest possible way Newtonian dynamics, providing an extremely powerful tool to address one of the most puzzling problem that modern astrophysics is facing: the true nature of the dark matter.

References

1. Sanders, R. H. 2010, *The Dark Matter Problem: A Historical Perspective*. Cambridge University Press, 2010.
2. Bertone, G., & Hooper, D. 2016, arXiv:1605.04909

3. Famaey, B., & McGaugh, S. S. 2012, *Living Reviews in Relativity*, 15
4. Sanders, R. H., & McGaugh, S. S. 2002, *ARA&A*, 40, 263
5. Milgrom, M. 2011, XXXV International Conference of Theoretical Physics "Matter to the Deepest". *Acta Physica Polonica B* vol. 42, 2175
6. Scarpa R., Marconi G., Carraro G., Falomo R., and Villanova S. 2011, *A&A* 525, 148
7. Scarpa R. and Falomo R. 2010, *A&A* 523, 43
8. Scarpa R., Marconi G., Gilmozzi R., Carraro G. 2007, *A&A* 462, L9
9. Scarpa R., Marconi G., and Gilmozzi R. 2003, *A&AL* 405, 15
10. Lane R. R., Kiss L. L., Lewis G. F. et al. 2009 *MNRAS* 400, 917
11. Lane R. R., Kiss L. L., Lewis G. F. et al. 2011 *A&A* 530, A31
12. Jiang and Tremaine 2010 *MNRAS*, 401, 977
13. Hernandez, X., Jiménez, M. A., & Allen, C. 2012, *European Physical Journal C*, 72, 1884
14. Milgrom, M. 1983a, *Apj*, 270, 365
15. Bekenstein, J. D. 2004, arXiv:astro-ph/0412652
16. Milgrom, M. 1983b, *Apj*, 270, 371
17. Milgrom, M. 1983c, *Apj*, 270, 384
18. Moffat, J. W. 2006, *JCAP*, 3, 4
19. Rodrigues, D. C., Letelier, P. S., & Shapiro, I. L. 2010, *JCAP*, 4, 20
20. Hehl F. W. & Mashhoon B. 2009, *Physics Letters B*, 673, 279
21. Shaya E. J. and Olling R. P., 2011, *ApJS*, 192, 2.
22. Perryman M. A. C., Lindegren L., Kovalevsky J. et al. 1997, *A&AL* 323, 49
23. Telting J. H., Avila G., Buchhave L. et al. 2014, *AN* 335, 41
24. Stemples 2005, FIES user manual <http://www.not.iac.es/instruments/fies/fiestool/>
25. Bertone, E., Buzzoni, A., Chavez, M., Rodriguez-Merino, L. H. 2008, *A&A* 485, 823
26. Kurucz R. L. 1995, *Highlights of Astronomy*, 10, 407